UWL REPOSITORY

repository.uwl.ac.uk

Developments in the use of ultra high performance fiber reinforced concrete as strengthening material

This is the Accepted Version of the final output.

1 **Developments in the use of Ultra High Performance Fiber Reinforced Concrete as**

2 **Strengthening Material**

3 **Dr Spyridon Paschalis[a*], Dr Andreas Lampropoulos[b]**

4 **[a] School of Engineering, Department of Civil Engineering, University of Bolton, UK**

5 **[b] School of Environment and Technology, University of Brighton, UK**

6 **Abstract**

7 Ultra High Performance Fiber Reinforced Concrete (UHPFRC) is a novel material which has

8 been developed the last few decades and has been applied in applications that require high

9 strength, ductility and durability. Recently, the material has been applied in strengthening

10 applications. The present study aims to investigate new techniques for the application of

11 UHPFRC as strengthening material and to provide an insight into the parameters affecting the

12 performance of elements strengthened with UHPFRC. The present research investigates for the

13 first time the effectiveness of the use of dowels at the interface between UHPFRC and concrete,

14 to improve the connection between these two materials. Additionally, the effectiveness of the

15 use of UHPFRC jackets for the strengthening of Reinforced Concrete (RC) beams has been

16 examined. In the present research, a systematic experimental study has been conducted together

17 with numerical study.

18 The results demonstrate that both examined techniques are effective and should be taken into

19 consideration when UHPFRC is applied for strengthening material. The dowels result in better

20 bonding at the interface and can delay the formation of cracks in the post elastic phase, leading

21 to reduced interface slip values and subsequent enhanced load bearing capacity. This technique

22 should be taken into consideration to eliminate the risk of premature de-bonding of the

23 strengthening layer. The construction of UHPFRC jackets on the other hand, results in a

24 dramatic increase of the stiffness and the load carrying capacity of the strengthened elements

25 and should be preferred in cases of heavily damaged RC members.

26 **Keywords**

27 Strengthening; Ultra High Performance Concrete; Full scale; Beams; UHPFRC jackets

28 **1. Introduction**

29   The structural upgrade of existing structures is a key priority worldwide. Nowadays, there

30 are many available strengthening techniques. However, the extensive preventative application

31 of these techniques for the protection of existing structures cannot be applied mostly due to

32 issues linked to difficulties during the application of the techniques, which require special

33 expertise, increased cost and construction time.

34   The present research focus on the application of an advanced material, such as the Ultra

35 High Performance Fiber Reinforced Concrete (UHPFRC), for the strengthening of Reinforced

36 Concrete (RC) members. The examined technique present crucial advantages which are related

37 to the enhanced properties of the material and durability, and ease of preparation and

38 application of the material. Another advantage of the examined technique is that thin elements

39 with high strength and ductility can be constructed and therefore the dimensions of the

40 strengthened elements do not change dramatically.

41   There are numerous published studies on the development and characterisation of the

42 mechanical properties of UHPFRC [1-7]. The fiber distribution is an important parameter

43 affecting the performance of UHPFRC and this was thoroughly investigated by Ferrara et al.

44 [1]. Nicolaides et al. [2], developed an optimum mixture of Ultra High Performance

45 Cementitious Composite with materials which were locally available in Cyprus, while

46 Paschalis and Lampropoulos [3], investigated the effect of fiber content and curing time

47 regimes on the tensile characteristics of UHPFRC. In this study it was found that the fiber

48   content significantly affects the tensile characteristics of UHPFRC, and different stress-strain

49   models for various typical fibers contents, were proposed. The mechanical characteristics of

50   UHPFRC under different loading conditions, including static and cyclic loading, have been

51   studied in previously published studies [4-7].

52   The application of UHPFRC for the retrofitting of existing RC members has also been

53   studied recently [8-12]. Bruhwiler and Denarie [8], applied UHPFRC in a series of

54   rehabilitation applications, such as in a road bridge, a bridge pier and an industrial floor. Al-

55   Osta et al. [9], studied the effectiveness of different techniques for the strengthening of RC

56   beams using prefabricated UHPFRC strips and comparisons were made with cast-in-situ

57   UHPFRC layers. Different strengthening configurations, such as strengthening on different

58   sides of the beams were also investigated in this study. Safdar et al. [10], applied UHPFRC as

59   a repair material and found that this application can increase mainly the stiffness of the

60   strengthened elements. Lampropoulos et al. [11], presented a numerical investigation on the

61   performance of UHPFRC for the flexural strengthening of RC beams and the effectiveness of

62   the technique was highlighted. Paschalis et al. [12], presented an experimental and numerical

63   investigation on the performance of UHPFRC for the flexural strengthening of full scale RC

64   beams. In this study, UHPFRC layers with and without the use of steel bars in the layers were

65   used for the strengthening of RC beams, and it was found that the UHPFRC layers can increase

66   the stiffness of the strengthened members, while the addition of steel bars to the layers can

67   produce a big increase of the load carrying capacity. Finally, a better bonding between

68   UHPFRC and concrete was identified compared to concrete to concrete interfaces. However,

69   in this study it was found that the slips at the interface were not negligible. On the contrary,

70   high values of slip at the interface were recorded in the post-elastic region.

71   Based on existing studies, the application of UHPFRC can be effectively used to

72   enhance the stiffness of the strengthened elements, while the load bearing capacity can also be

further increased with the addition of steel bars. However, the addition of steel bars is a labour-intensive technique and requires a minimum thickness for the strengthening layer leading to significant changes in the geometry and the characteristics of the initial structure.

The present study aims to investigate new techniques for application of UHPFRC as strengthening material with the optimum result and to provide an insight into the key parameters affecting the structural performance of strengthened elements with UHPFRC. Therefore, the present research investigates for the first time the effectiveness of the use of dowels at the interface between UHPFRC and concrete, to improve the connection between these two materials and to eliminate the risk of premature de-bonding. Also, in the present study the effectiveness of the use of three-side UHPFRC jackets has been examined. Both techniques aim to upgrade the structural performance of the existing elements without the use of steel bars in the strengthening layers/jackets. The application of this technique could be easily applied in strengthening applications reducing labouring cost and effort [13-15].
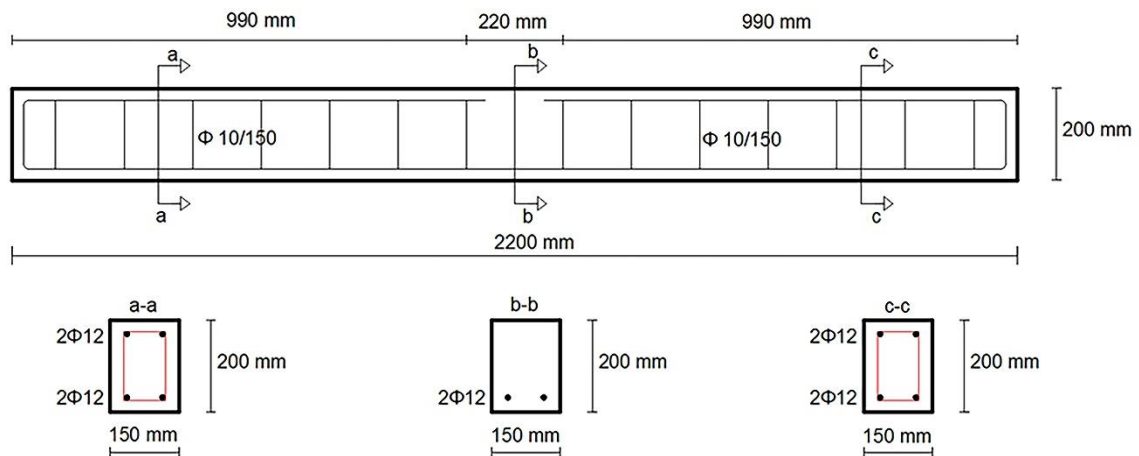
2. Experimental program

2.1 Strengthening techniques

Eight RC beams have been examined in the present research. Two beams were used as control beams without any retrofit, two beams were strengthened with UHPFRC layers without dowels and another two identical beams were strengthened with UHPFRC layers and dowels at the interface. Finally, two beams were strengthened with three-side UHPFRC jackets (Table 1). In all the strengthened beams the surfaces of the initial beams were roughened prior to the casting of the UHPFRC layer.

96　**Table 1** Examined Beams

Beam	Strengthening Technique
P1	Control beam
P2	Control beam
U1	UHPFRC layer
U2	UHPFRC layer
D1	UHPFRC layer and dowels
D2	UHPFRC layer and dowels
3SJ1	UHPFRC Jacket
3SJ2	UHPFRC Jacket

97

98　　　　The initial beams (Figure 1) were reinforced using two steel bars grade B500C with 12

99　mm diameter at the tensile side. Also, shear links of the same steel grade with 10 mm diameter

100　were placed at 150 mm spacing along the length of the beam.

101

102　**Fig. 1** Geometry and reinforcement of the RC beams

103　　　　The layers had a depth of 50 mm, a breadth of 150 mm (equal to the breadth of the initial

104　beam) and were cast along the whole length of the tensile side of the beams. As can be seen in

105　Figure 2a, ribbed steel bars with a length of 126 mm, in total, 12 mm diameter and a spacing

106　of 222 mm were used as dowels. The design of dowels was based on the Greek Retrofitting

107 Code [16]. When steel bars are used as dowels, the minimum required cover in the direction of

108 loading should be at least $5d_b$ for the front cover and $6d_b$ at the back cover (where d_b is the

109 diameter of the bars) to prevent premature failure of the concrete edges around the dowels [16].

110 On the vertical direction, a cover of at least $3d_b$ is required, while it is also suggested that the

111 length of the bars inside concrete should be at least $8d_b$ [16]. In Figure 2b, the position of the
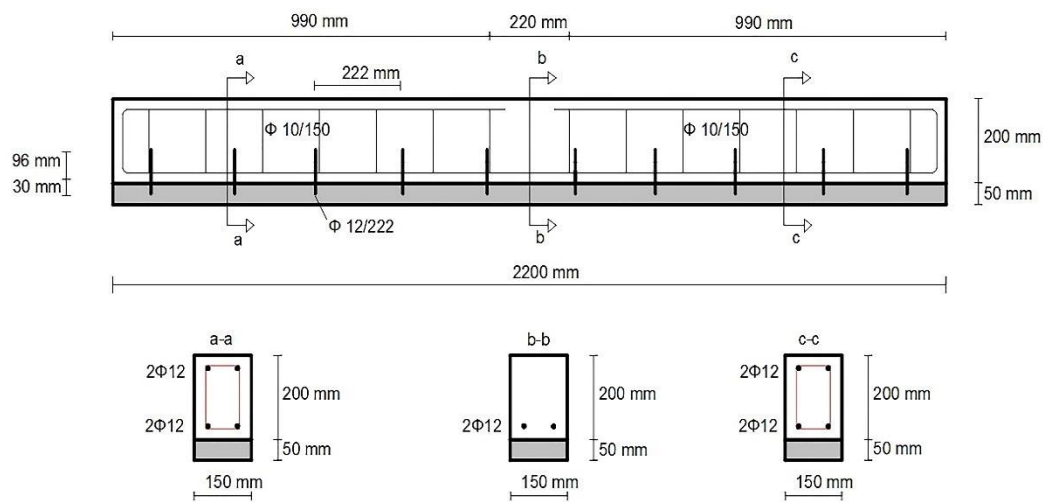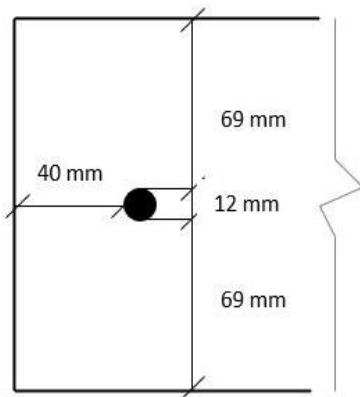
112 dowels is presented

113

114 **Fig. 2a**

115

116 **Fig. 2b**

117 **Fig. 2** a) Geometry and reinforcement of the strengthened beams with layers and dowels b)

118 Position of the dowels

119   The strengthening technique and the geometry of the strengthened beams with

120   UHPFRC jackets on three sides is presented in Figure 3.
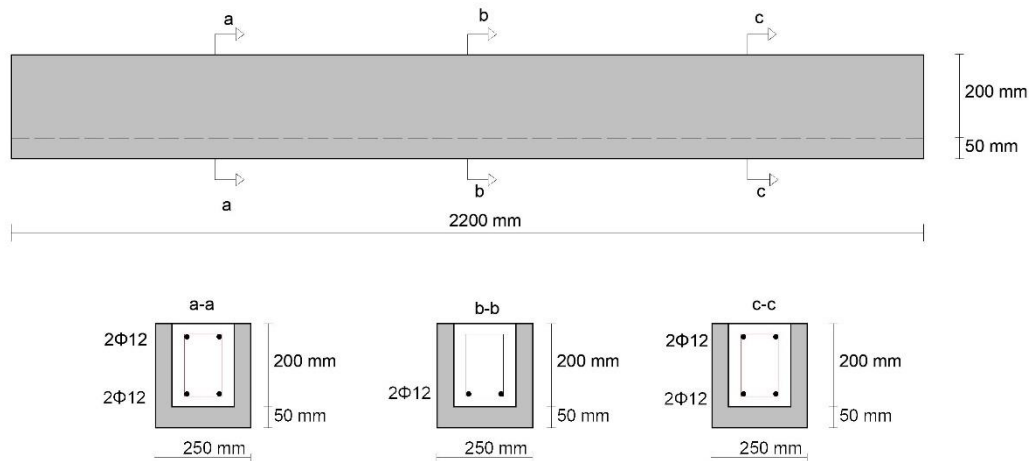

121

122   **Fig. 3** Strengthening with three-side jackets

123   As can be seen in Figure 3, a thickness of 50 mm was used for the UHPFRC jacket

124   leading to a beam with total breadth equal to 250 mm and a height of 250 mm. The jackets

125   were cast along the full length of the beams.

126   **2.2 Preparation of the specimens**

127   For the preparation of the UHPFRC, fine sand with a maximum particle size of 500 μm

128   was used together with microsilica, Ground Granulated Blast Furnace Slag (GGBS) and high

129   strength cement class 52.5 R type I. In addition, steel microfibers with a length of 13 mm and

130   a diameter of 0.16 mm were incorporated in the mix.

131   According to study [17], a fiber content in the range of 3-4 Vol-%, is considered an

132   optimum content for the preparation of the UHPFRC considering parameters such as; the

133   rheological properties, the performance of the material and the cost. Therefore, in the present

134   study a fiber content of 3 Vol-% was adopted. The mixture design of UHPFRC is presented in

135   Table 2 and the mixture design of the conventional concrete is presented in Table 3.

Table 2 The mixture design for the preparation of UHPFRC

Material	Mix proportions (kg/m^3)
Cement	620
GGBS	434
Silica fume	140
Silica Sand	1051
Superplasticizer	59
Water	185
Steel fibers	235.5 (3 Vol.-%)

Table 3 The mixture design for the preparation of concrete

Material	Mix proportions (kg/m^3)
Cement	340
Fine Aggregates	1071
Coarse Aggregates	714
Water	205

The initial beams were wet cured daily for 28 days. A pistol grip needle scaler was employed and all the strengthened beams were roughened to a depth of 2-2.5 mm. To quantify the surface texture, the sand patch method was used [12]. Once the desired roughening depth was achieved and the surface was ready, the beams were drilled, using an impact drill, and the dowels were placed in position. Based on Technical Specifications on the placement of dowels in concrete elements [18], when steel bars are used as dowels, it is suggested that the diameter of the hole (d_h) should be 4 mm higher than the diameter of the connectors (d_b).

161   For the connection of the dowels with the beams, a thixotropic structural two-part

162   adhesive was used. According to the specifications from the manufacturer, the compressive

163   strength of the epoxy over 14 days at +15°C was 70-80 MPa, while the tensile strength was in

164   the range of 25-28 MPa.

165   Before the application of the jackets on the other hand, the beams were roughened on

166   all the three sides. Once the coating was removed and the desired depth was achieved, the

167   beams were cleaned carefully before the casting of the jackets.

168   The UHPFRC layers and jackets were applied two months after the casting of the initial

169   beams and the strengthened beams were tested after four months. In Figure 4, the procedure

170   for the preparation of the strengthened beams with layers and dowels (Figure 4a and 4b) and

171   jackets (Figure 4c) is presented.

172

173

174

175

176

177

178

179

182

Fig. 4a   **Fig. 4b**   **Fig.4c**

Fig. 4 a) Drilling of the initial RC beam b) dowels in place c) roughened beam on 3 sides

2.3 Properties of the materials

Three cubes of 100 mm side were tested to identify the compressive strength of both conventional concrete and the UHPFRC. The compressive tests were conducted following the BS EN 12390-3:2009 [19]. The samples were obtained from the same batch with the examined specimens, water cured at ambient temperature for 28 days and tested the same day with the testing of the beams. The average compressive strength of the conventional concrete cubes was

191   30.9 MPa and the standard deviation was found to be equal to 2.34 MPa. The average

192   compressive strength of the UHPFRC on the other hand, was found to be equal to 136.5 MPa

193   and the standard deviation was 5.5 MPa.

194   The tensile properties of the UHPFRC were evaluated using six dog-bone shaped

195   specimens (Figures 5a-b). Tests were conducted under constant loading with a displacement

196   rate of 0.007 mm/sec, which is the same loading rate has been used in other studies [3,4,12]

197   leading to comparable results. The tensile stress-strain results are illustrated in Figure 5c. From

198   the average curve, the maximum stress was found to be equal to 11.5 MPa, the elastic limit was

199   5 MPa and the modulus of elasticity was calculated equal to 51 GPa. All the specimens were

200   tested the same day with the strengthened beams.

201

202
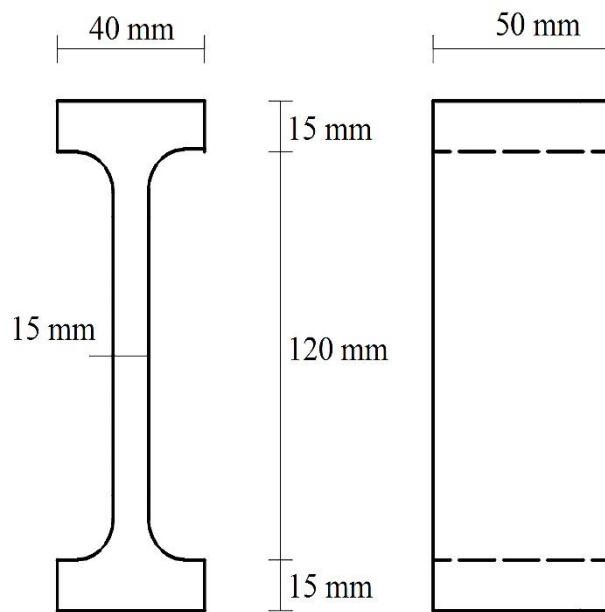
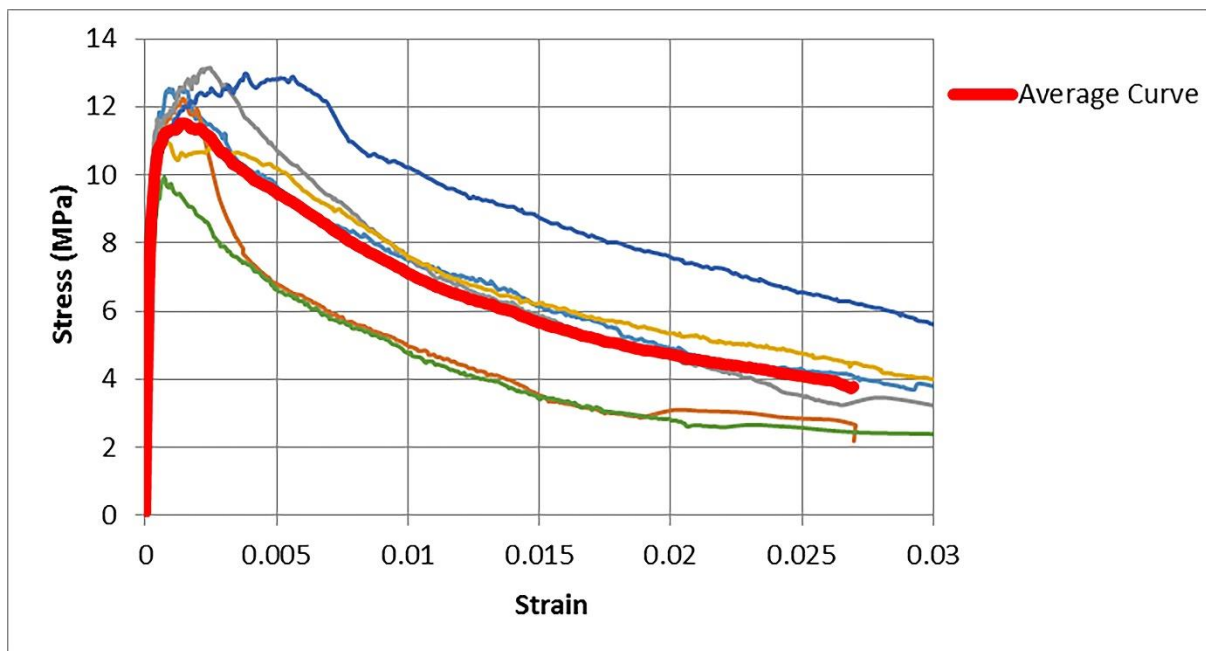203   **Fig. 5a**

204

205

Fig. 5b

207

208

Fig. 5c

Fig. 5 a) Dog bone specimen before Testing b) Dimensions of the Dog bone Specimen c)

Experimental results from the direct tensile tests of UHPFRC

212   **2.4 Testing of the beams**

213   The examined beams, were tested under a four-point loading test with a displacement

214   rate of 0.008 mm/sec, which is in agreement with the loading rate used by other researchers

215   [12,22] leading to comparable results The experimental setup for the examined beams is

216   presented in Figures 6 a-d.

217

218   **Fig. 6a**

219

220   **Fig. 6b**

221

222   **Fig.6c**

223

Fig.6d

Fig. 6 Experimental setup for the a) control beam b) strengthened beam with layers c)

strengthened beam with layer and dowels d) strengthened beam with jacket

During the testing of the strengthened beams with layers, apart from the load carrying

capacity and the deflection, the slips at the interface between UHPFRC and RC were recorded

using nine Linear Variable Differential Transformers (LVDTs) in total. As can be seen in

Figures 7a and 7b, six LVDTs were placed on side 1 along the full length of the beam, while

three LVDTs were placed at the second side to validate the results obtained from side 1.
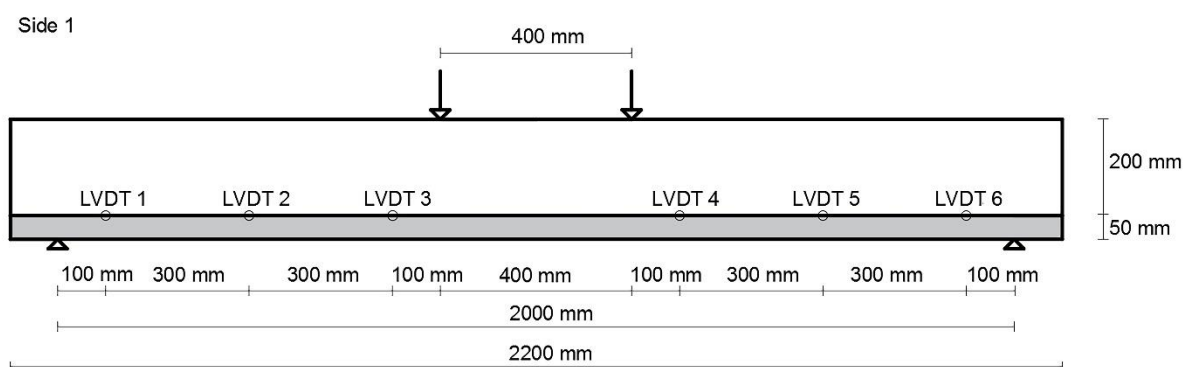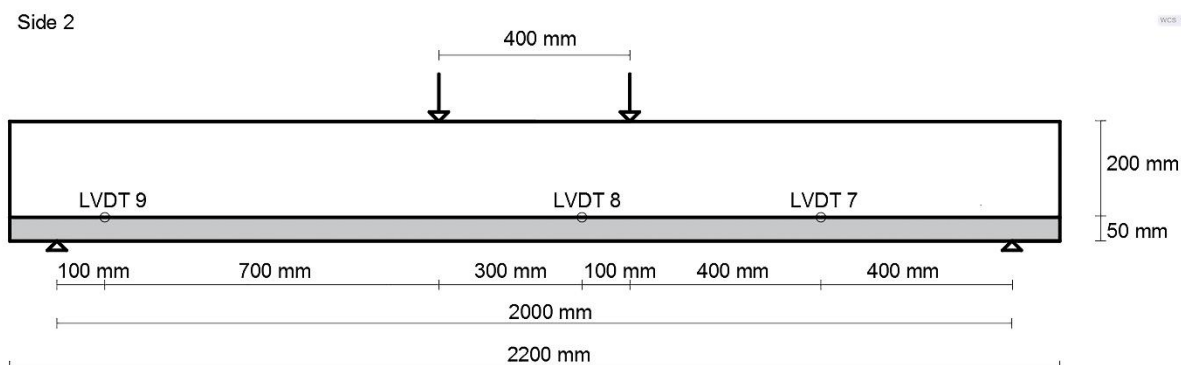

233

Fig. 7a

235

Side 2

400 mm

200 mm

LVDT 9   LVDT 8   LVDT 7

50 mm

100 mm   700 mm   300 mm 100 mm   400 mm   400 mm

2000 mm

2200 mm

236

237 **Fig. 7b**

238 **Fig. 7** a) Positions of the LVDTs for the measurement of slips on side 1 b) positions of the

239 LVDTs for the measurement of slips on side 2

240 **2.5 Experimental results of the examined beams and discussion**

241   The experimental results for the control beams, the strengthened beams with UHPFRC

242 layers, the strengthened beams with UHPFRC layers and dowels and the strengthened beams

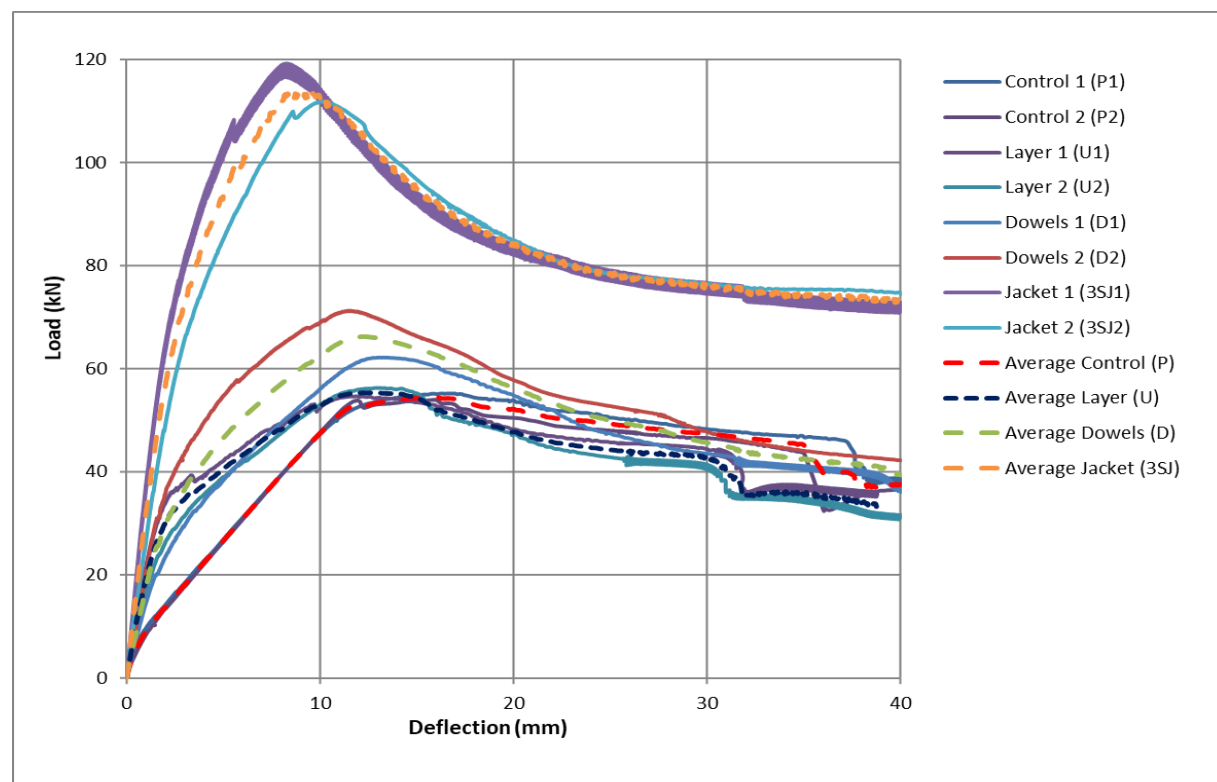243 with jackets are presented in Figure 8.

244

245 **Fig. 8** Experimental results for all the examined beams

246   The average load-deflection results, for all the examined beams, are presented in the same

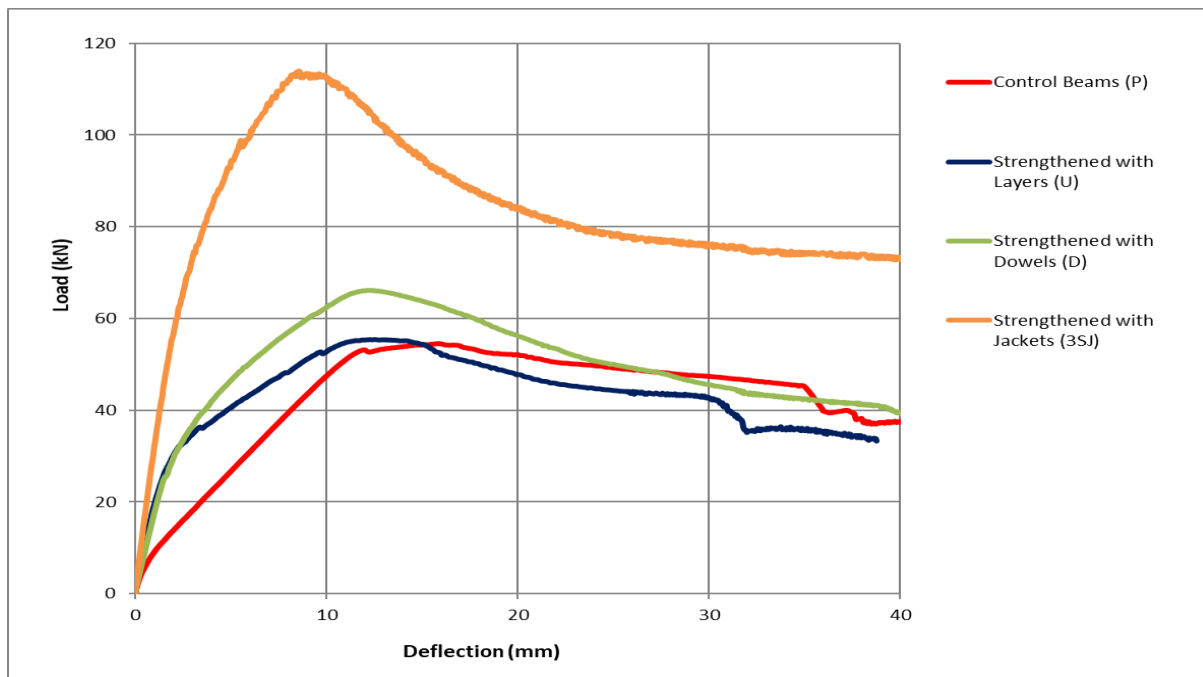247   graph in Figure 9.

248

249   **Fig. 9** Average load-deflection results

250   From Figure 9, the end of the linear part for each configuration was identified and is

251   representing the formation of significant cracks, and the values are presented in Table 4. In this

252   table, the average values for the maximum load, the stiffness and the displacement at the

253   maximum load are also presented.

254   **Table 4** Maximum load and Stiffness for all the examined beams

Beam	Maximum load (kN)	Stiffness (kN/mm)	Start of Cracking (kN)	Displacement At Peak Load (mm)
Average P1,2	54.6	9.2	5	15.8
Average U1,2	55.3	21.5	15	12.3
Average D1,2	66.2	18.3	24	12
Average 3SJ 1,2	114.5	34	58	8.6

255

256   The results of Figure 8, show a small scatter of the results of the identical samples. As

257   illustrated in this figure, similar values were achieved for the maximum load of beams P1 and

258   P2 (55.1 kN for beam P1 versus 54 kN for beam P2) and the stiffness (10.5 kN/mm for beam

259   P1 versus 8.4 kN/mm for beam P2). Considering the average load-defection curve, the

260   maximum load was found to be equal to 54.6 kN, the stiffness was calculated to be 9.2 kN/mm

261   and the deflection at the maximum load was equal to 15.8 mm.

262   The load-deflection results obtained for the identical beams U1 and U2 are also presented

263   in the same graph in Figure 8. From this figure, it is clear that there is a positive agreement in

264   the experimental results for both the identical beams in terms of maximum load (54.6 kN for

265   beam U1 versus 56.3 kN for beam U2) and the stiffness (23 kN/mm for beam U1 versus 19.2

266   kN/mm for beam U2). Based on the average load-deflection curve, the maximum load was

267   found to be equal to 55.3 kN, the stiffness was calculated to be equal to 21.5 kN/mm and the

268   deflection at the maximum load was equal to 12.3 mm.

269   From Figure 8, it can also be noticed that the load carrying capacity of beam D2 (71.3

270   kN) and the stiffness (21 kN/mm), were higher compared to the respective values of beam D1

271   (62.2 kN the maximum load and 16.5 kN/mm the stiffness), which is attributed to imperfections

272   during the preparation of the samples and during the installation of the dowels. However, both

273   beams exhibited higher load carrying capacity compared to beams U1 and U2. Considering the

274   average curve, the maximum load was found to be equal to 66.2 kN, the stiffness was 18.3

275   kN/mm and the deflection at the maximum load was equal to 12 mm.

276   From Figures 8 and 9, a big increase in the load the load carrying capacity and the

277   stiffness of the strengthened beams with jackets can be distinguished, compared to all the other

278   techniques. The maximum load of beam 3SJ1 was found to be equal to 119.2 kN and the

279   stiffness was calculated to be equal to 38.8 kN/mm. The maximum load of beam 3SJ2 on the

280   other hand, was found to be equal to 112 kN and the stiffness 30.5 kN. Considering the average

281   curve, the maximum load was equal to 114.5 kN, the stiffness was 34 kN/mm and the deflection

282   at the maximum load was equal to 8.6 mm.

283   Considering the average results of Figure 9 and Table 4, it is clear that in all the examined

284   cases the stiffness of the strengthened members was significantly enhanced. Based on the

285   results of the present investigation, the contribution of UHPFRC layers without the use of

286   dowels or any other reinforcement, relies mainly on the delay of the formation of cracks and

287   the significant stiffness enhancement. Based on the average results of Table 4, strengthening

288   with UHPFRC layers resulted in significant stiffness increment (134%), while the load capacity

289   was only slightly increased by 1.5% . These results are also in agreement with other studies in

290   the literature review [10,12]. In these studies it was highlighted that the main contribution of

291   UHPFRC layers is on the delay of the formation of cracks and the significant increment of the

292   stiffness. On the contrary, the contribution UHPFRC layers in the load carrying capacity is

293   lower.

294   From Figure 9 and Table 4, it can also be observed that the addition of dowels, apart

295   from the increment of stiffness, resulted in a significant enhancement of the load bearing

296   capacity of the strengthened beams. More specifically, an average increment of 21.5% was

297   identified in this case. On the contrary, the average increment in the load carrying capacity of

298   the strengthened beams U1, U2 was only 1.5%.

299   During the testing of the strengthened beams with UHPFRC layers and dowels, it was

300   observed that the formation of cracks was delayed compared to the strengthened beams with

301   UHPFRC layers only. This was obvious from the visual inspection of the beams during the

302   testing, and was also reflected to the load-deflection results. From the results of Table 4 it is

303   clear that the addition of dowels at the interface had as a result the delay in the formation of

304   the cracks compared to the strengthened beams without dowels. When dowels were placed at

305 the interface between RC and UHPFRC, cracking was initiated at a load value 60% higher

306 compared to the beams with UHPFRC layers without dowels.

307   The results of the present investigation also indicate that the construction of jackets on

308 three sides is also a very effective strengthening technique which can improve the performance

309 of the strengthened members. From Figure 9 and Table 4, it can be seen that the addition of

310 jackets on three side resulted to a remarkable increment of both the stiffness and the load

311 carrying capacity of the strengthened members. In this case, the maximum load was increased

312 by 110% and the stiffness was enhanced by 270%. It can also be seen that the formation of

313 cracks was initiated at a value of load 334% higher compared to the beams strengthened with
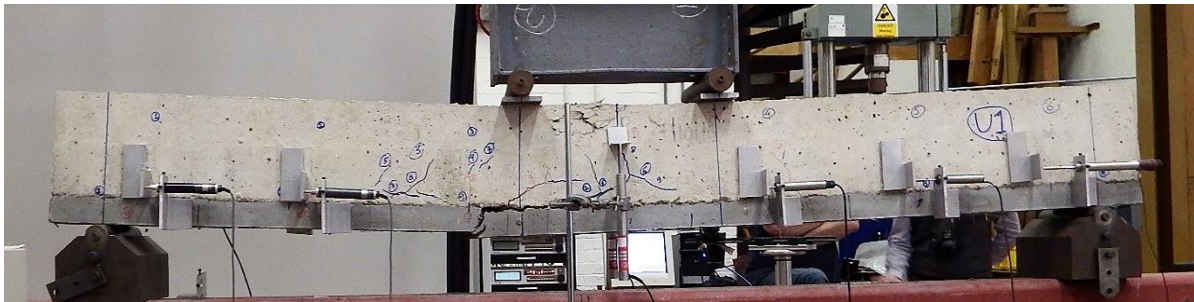
314 UHPFRC layer only.

315   In the literature there are limited applications of jackets for strengthening of RC

316 members. Al-Osta et. [9] investigated different configuration such as strengthening on one side,

317 on two sides and three sides. The biggest load increment (89%) was noticed when three sides

318 jacket was applied. In the present study, the biggest load carrying capacity was also identified

319 for strengthening with UHPFRC jackets, but with a higher increment of 110%.

320   In comparison with other strengthening techniques in the literature using UHPFRC, the

321 addition of three-side jacket appears to be the most effective in terms of structural performance.

322 Paschalis et al [12], used steel bars in the UHPFRC layers as extra reinforcement for the

323 strengthening of existing RC beams at the tensile side. The geometry of the beams and layers,

324 and the material properties in this study were the same with the present study. The results

325 showed an increment of 89.5% on the maximum load and 111% on the stiffness of the

326 examined beams. These values are lower compared to the jacketed beams, where increment of

327 110% on maximum load and 334% on the stiffness were achieved.

328

329   In Figures 10a-f the failure mode of the examined beams is presented.
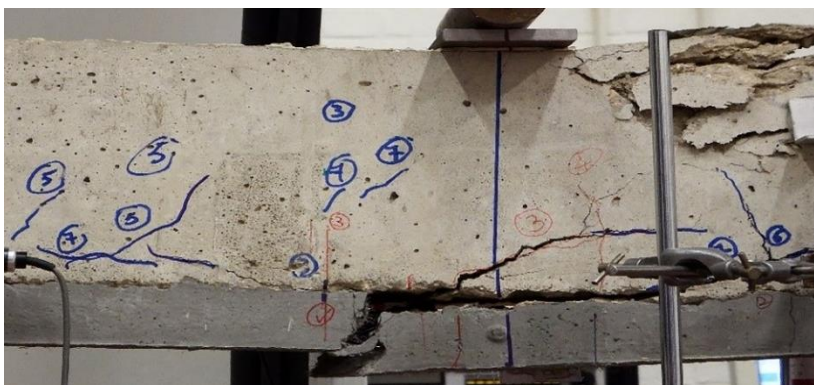

330

331   **Fig. 10a**

332

333   **Fig. 10b**

334

335   **Fig. 10c**

336
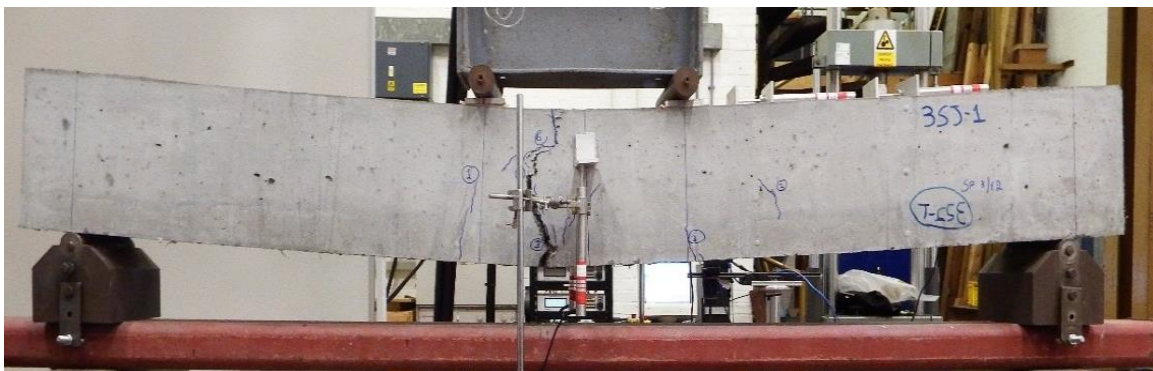
337   **Fig. 10d**

Fig. 10e

Fig. 10f

Fig. 10g

Fig. 10 Beams at failure: a) control beam P1 b) strengthened beam with UHPFRC layers U1 c) strengthened beam with UHPFRC layers U2 d) local de-bonding at the interface of beam U1 e) strengthened beam with dowels D1 f) bonding at the interface of beam D1 g) strengthened beam with jacket 3SJ1

349   The failure mode of the control beams P1 and P2 was identical and was characterized by

350   flexural cracks (Figure 10a). A single crack appeared initially in the middle of the span

351   followed by additional cracks which propagated towards the supports. Inclined shear cracks

352   appeared at a later stage, followed by the crushing of the compressive side at the middle of the

353   span which occurred in the descending branch of the load-deflection curve.

354   The failure of the beams which were strengthened with UHPFRC layers only, started

355   with a major flexural crack which was initiated at the UHPFRC layers and propagated

356   progressively to the RC beams. Additional minor cracks appeared near the interface during the

357   testing. As can be seen in Figures 10 b-c less cracks appeared in these beams compared to the

358   control beams. However, during of the testing of beam U1, a local de-bonding at the interface

359   between UHPFRC and concrete started when the load reached a value of 48 kN and before the

360   maximum load carrying capacity (Figure 10d). After post-testing inspection of the specimen,

361   it was observed that parts of the interface of this specimen had lower roughness depth, therefore

362   the premature failure of this specimen is attributed to the insufficient interface treatment. On

363   the contrary, the bonding at the interface of beam U2 was effective (Figure 10c), and in this

364   case de-bonding was prevented and typical flexural failure occurred at the middle of the span

365   length, followed by crushing of the compressive side.

366   The failure mode of beams D1 and D2 was identical. The dowels resulted in a strong

367   bonding between UHPFRC and concrete and de-bonding was prevented in both cases. The

368   specimens failed with a single flexural crack in the middle of the span. These cracks appeared

369   on the UHPFRC layer and progressively propagated to the RC beam resulted in the failure of

370   the beams. Additional minor inclined cracks appeared during the testing of the beams (Figure

371   10e). Crushing of the compressive side occurred at the post peak load-deflection region. In

372   Figure 10f it can be seen that one single crack started from the layer and propagated at exactly

373   the same position of the RC beam. This shows very good connection at the UHPFRC-to-

374   concrete interface which is attributed to the addition of dowels. The enhancement of the

375   interface connection and the prevention of de-bonding which was achieved in this case shows

376   the beneficial contribution of the dowels. This needs to be considered in real life strengthening

377   applications where interface treatment imperfections may exist and this may lead to de-bonding

378   and failure of the elements as occurred in specimen U1.

379   Beams 3SJ1 and 3SJ2 which were strengthened with jacket on three sides, failed in a

380   similar way with a main flexural crack at the tensile side. As can be seen in Figure 10g, the

381   position of the major crack of beam 3SJ1 was in the middle of the span length. Beam 3SJ2 on

382   the other hand, failed in the position of close to the loading point. After post testing inspection

383   of this specimen, it was found that at this position the steel fibers were not evenly distributed

384   which may have resulted in failure at this point.

385   To further investigate the crucial topic of the bonding between UHPFRC and concrete,

386   measurements of the slips at the interface in different positions, were also recorded during the

387   testing of the strengthened beams (Figure 7). As aforementioned, a local de-bonding at the

388   interface of beam U1 occurred, and for this reason, the measurements of this beam were

389   ignored. The load versus interface slip results in different positions of beam U2 are presented
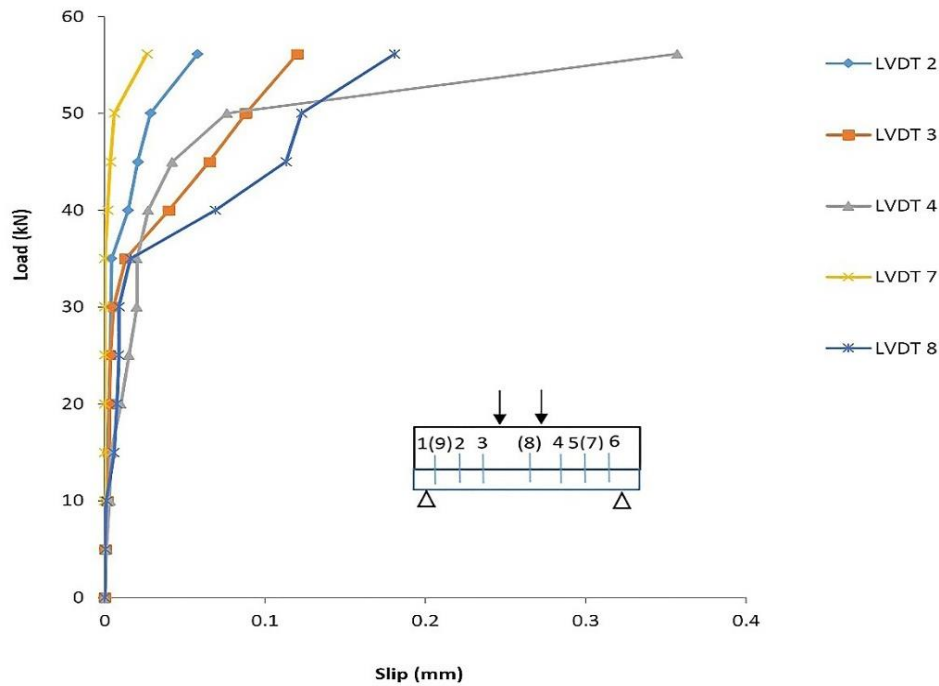
390   in Figure 11.

391

Fig. 11 Load versus slip in different positions for beam U2

As can be seen in Figure 11, slips were recorded at the positions of the LVDTs 2, 3, 4, 7 and 8, while for all the other positions negligible values were recorded indicating good connection (and therefore these points are not included in Figure 11). The maximum value of slip was recorded at the position of LVDT 4 with 0.36 mm (where the shear is maximum), while a value of 0.18 mm was recorded at the position of LVDT 8, which is located between the two loading points. Values in the range of 0.03-0.12 mm were recorded at the positions of LVDTs 2, 3 and 7. Zero values were recorded at the positions close to supports, as expected, due to the high shear strength at these points resulting from the support reactions.

The measurements of the slips at the interfaces of beams D1 and D2 are presented in Figures 12a and 12b.
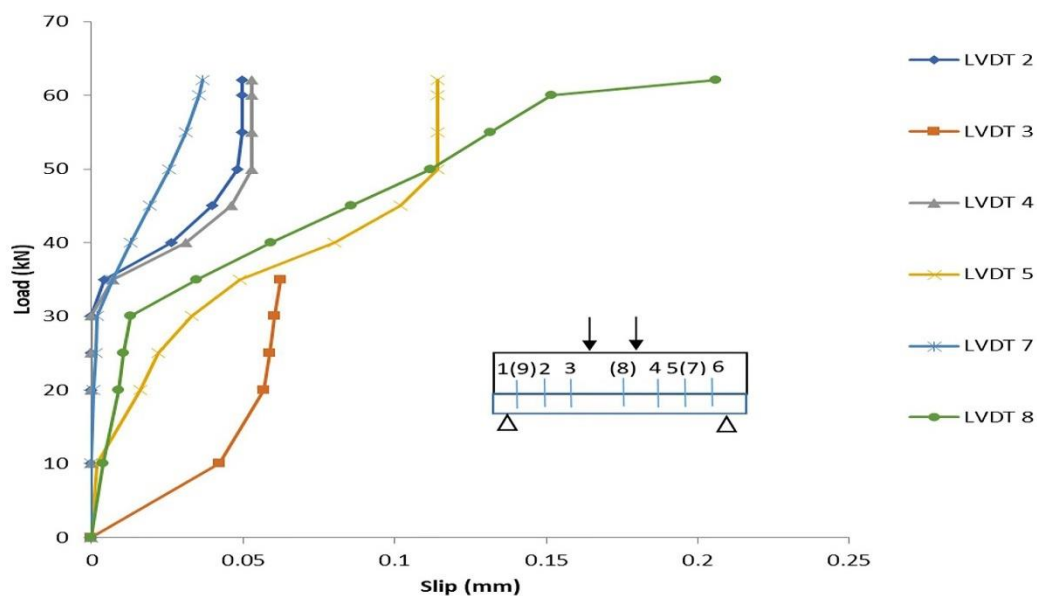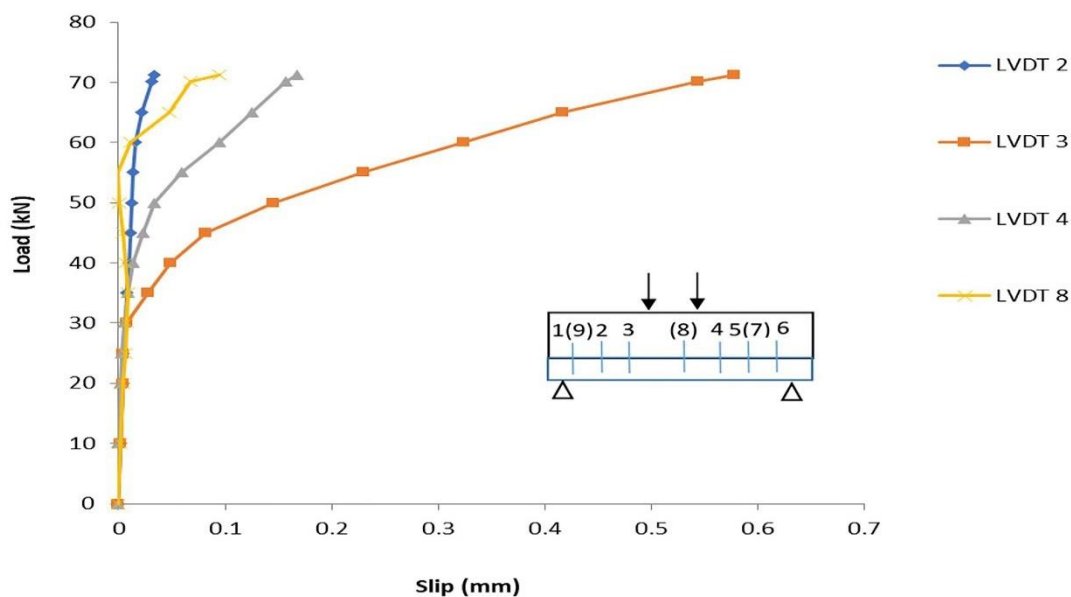
403

Fig. 12a

405

406

Fig. 12b

Fig. 12 a) Load versus slip in different positions for beam D1 b) load versus slip in different positions for beam D2

As shown in Figure 12a, the maximum value of slip of beam D1 was recorded at the position of LVDT 8, located between the two loading points, while only negligible slip values were recorded at the area close to the supports (and these points are not presented in Figure

413 12a). By contrast, values between 0.036 mm and 0.055 mm were recorded at the positions of

414 LVDTs 2, 4 and 7. Due to the fact that the metal angle section which supported LVDT 3 was

415 detached from the beam at a load value of 35 kN, these measurements are missing.

416   The measurements of slips at the interface of beam D2 are presented in Figure 12b. As

417 can be seen, slips were recorded only at the positions of LVDTs 2,3,4 and 8. Small values of

418 0.033 mm and 0.088 mm were recorded at positions 2 and 8 respectively. The highest values

419 of slip were recorded at the positions 3 and 4. It is worth mentioning that the failure of the beam

420 occurred in the area near the position of LVDT 3, leading to higher readings at this point.

421   A comparison between the recorded values of slip of beams U2, D1, D2 for a load value

422 equal to the maximum load of beam U2 (56.3 kN) is presented in Table 5.

423 **Table 5** Slip measurement for the beams U2, D1, D2 for value of load 56.3 kN

Position	Beam U2	Beam D1	Beam D2
LVDT 2	0.06	0.04	0.01
LVDT 3	0.11	0.01	0.19
LVDT 4	0.357	0.05	0.06
LVDT 7	0.03	0.03	0
LVDT 8	0.18	0.14	0.01

424   The result of Table 5 indicate that the recorded values of slip at beams D1 and D2 were

425 significantly lower compared to the respective values of beam U2 in almost all the examined

426 positions. Based on these results, it can be seen that only the recordings of LVDT 3 of beam

427 D2 were slightly higher than the respective values of U2 beam, which is attributed to the local

428 failure of the beam at this point.

429   Existing codes [20, 21] set limit values for different performance levels. The Greek

430 Code of Interventions [20], proposes a maximum slip value of 0.2 mm for the immediate

431 occupancy performance level, 0.8 mm for the life safety performance level and 1.5 mm and the

432 collapse prevention performance level. All the recorded values in the present study are lower

433 than 0.8 mm, which corresponds to the life safety prevention level. It is worth noticing that

434 most recorded values of the strengthened beams with dowels, are lower than 0.2 mm and only

435 in the position of LVDT3 of beam D2, which was affected by the failure of the beam in this

436 area, a higher value was recorded. According to the fib Bulletin 43 [21] on the other hand, a

437 maximum interface slip of 0.2 mm is suggested for the serviceability limit state and 2.0 mm

438 for the ultimate limit state.

439 In the literature there are recorded slip values for concrete to concrete interfaces in case

440 of beams strengthened with conventional concrete layers. Tsioulou et al [22], reported a

441 maximum value of slip of 1.1 mm for conventional concrete to concrete interfaces. In this

442 study, RC beams strengthened with RC layers without the use of dowels at the interface. This

443 value is significantly higher compared to the recorded values of the present investigation for

444 UHPFRC to concrete interfaces and according to Greek retrofitting code corresponds to

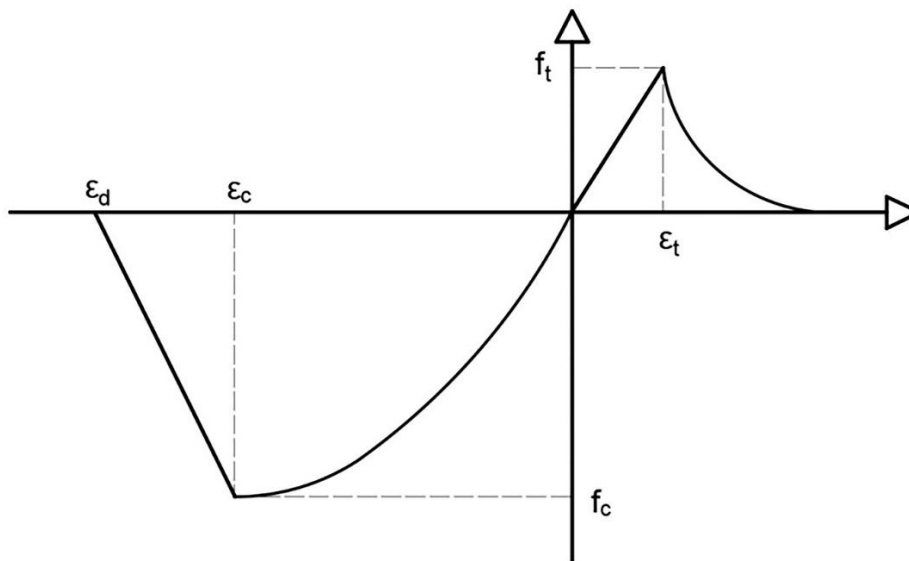445 collapse prevention performance level.

446 The results of the present experimental investigation indicate that the use of dowels at

447 the interface is an effective technique which should be taken into consideration when UHPFRC

448 layers are used for the structural upgrade of existing RC structures. The use of dowels delay

449 the formation of the cracks and result to lower slip values and higher load carrying capacity.

450 **3. Numerical modelling of the examined technique**

451 **3. 1 Modelling of the technique**

452 To further investigate the crucial topic of the effect of the interface conditions on the

453 performance of the strengthened elements a numerical investigation has been conducted.

454 Concrete was modelled with an eight-node element using the SBETA constitutive model [23].
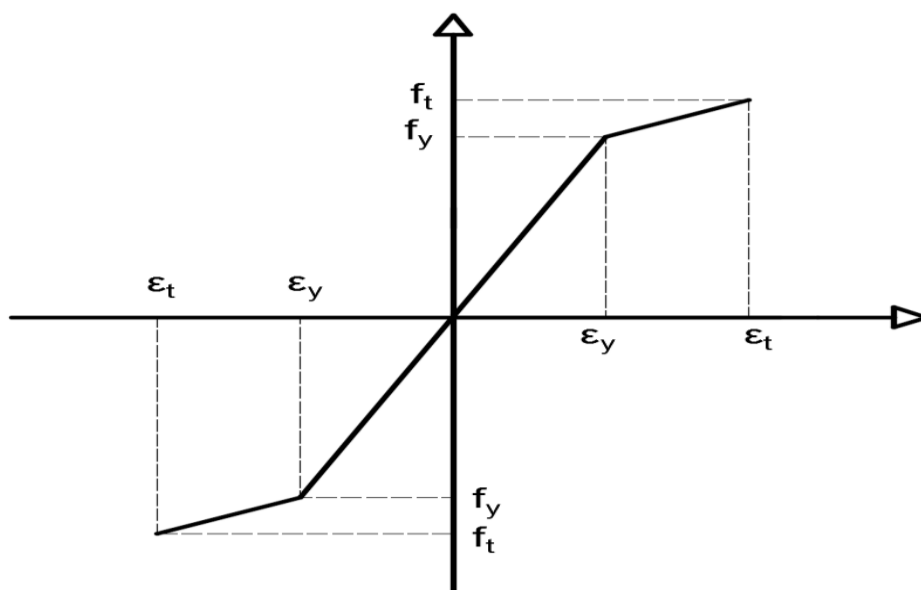
455   In Figure 13, the model used to simulate the behaviour of concrete in tension and compression,

456   is presented.

457

458   **Fig.13** Constitutive model in tension and compression adopted in ATENA software

459   The steel bars were simulated using linear elements with bi-linear behavior and

460   hardening, as presented in Figure 14. The properties of steel grade B 500C, according to BS

461   4449:2005 [24] were adopted for the modelling of the steel bars, while the cover of the steel

462   bars was the same as the experimental investigation.

463

464   **Fig. 14** Stress-strain model of the reinforcement

465   The concrete to steel bars bond was also taken into consideration. More specifically,

466   the CEB-FIB model code 90 [25] bond-slip model was adopted for the numerical modelling.

467   The interface between UHPFRC and concrete was modelled using two dimensional

468   contact elements with a coefficient of friction equal to 1 and cohesion 1.8 MPa, which were

469   determined using experimental data from a previously published study [12]. For the numerical

470   modelling of the strengthened beams with dowels, perfect connection at the interface was

471   considered.

472   For the modelling of the UHPFRC, the compressive and tensile characteristics obtained

473   experimentally were adopted. In compression, SBETA constitutive model [23] was used, while

474   for the modelling of the performance of the material in tension, the average stress-strain results

475   of Figure 5b were used. Based on these results, the response of the material in tension was

476   considered linear up to a value of stress level equal to 5 MPa, while a second part, up to the

477   maximum point, was used to model the strain hardening. After the ultimate stress, there is the

478   strain softening phase which was modelled with a bi-linear model. The model adopted in

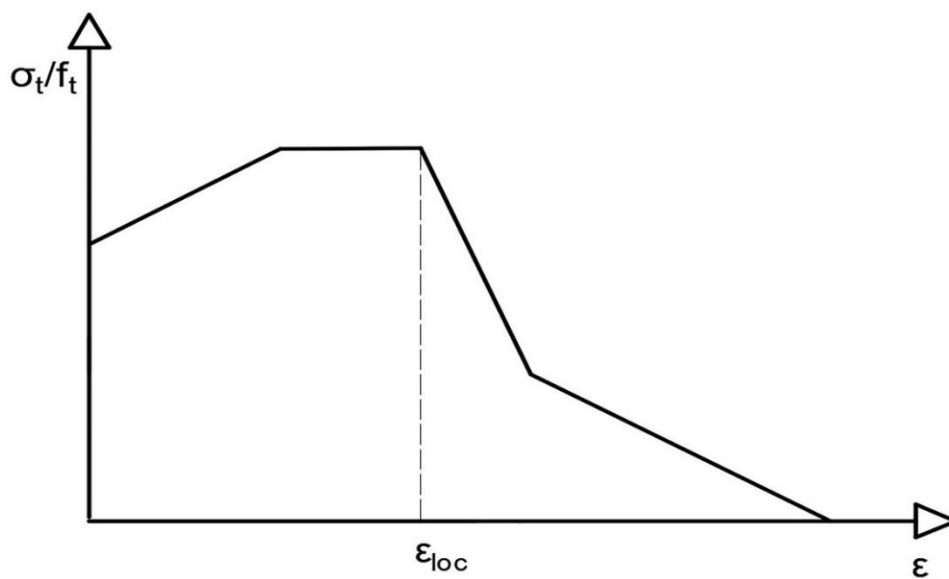479   tension is presented in Figure 15.

480

Fig.15 Tensile function adopted in ATENA software for the UHPFRC

482   For the modelling of the UHPFRC, the shrinkage was also taken into consideration

483   using a negative volumetric strain value to the UHPFRC elements. Based on existing study in

484   the literature review [3], an ultimate value of shrinkage equal to 565 microstrain was recorded

485   for a fiber content of 3% and this value applied to the UHPFRC layers.

486   **3.2 Validation of the numerical model**

487   A comparison between the average experimental and numerical results of the control

488   beam (P), the strengthened beams with UHPFRC layers without dowels (U), the strengthened

489   beams with dowels (D) and the strengthened beams with jackets ((3SJ) are presented in Figures
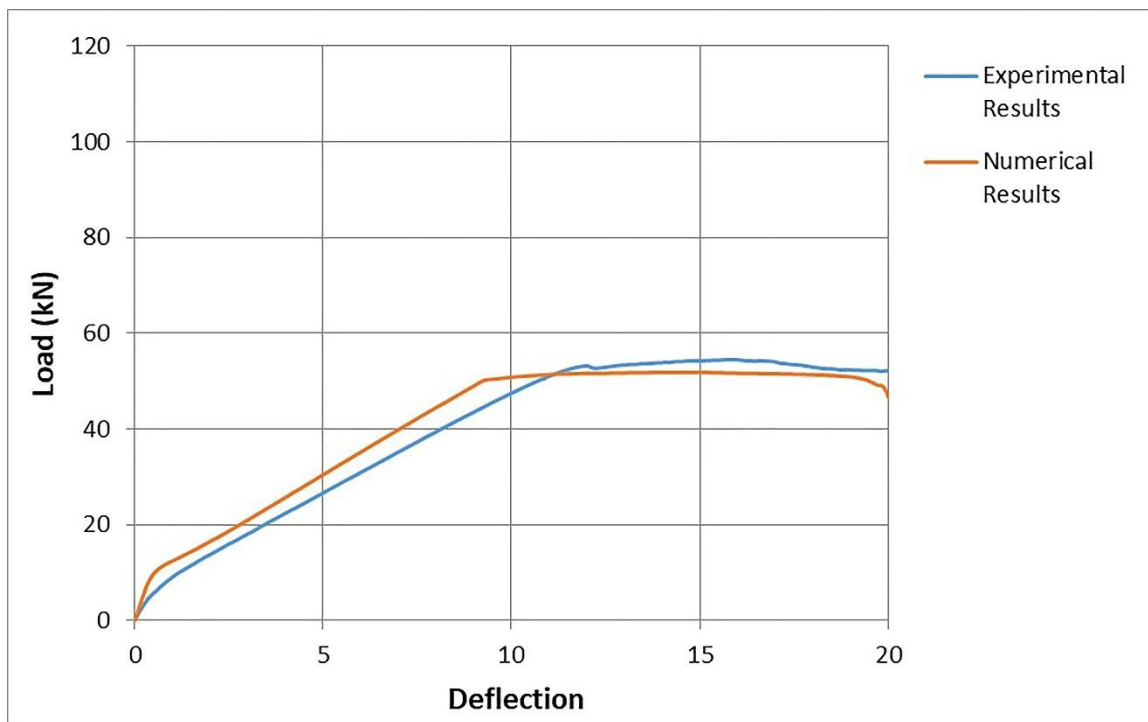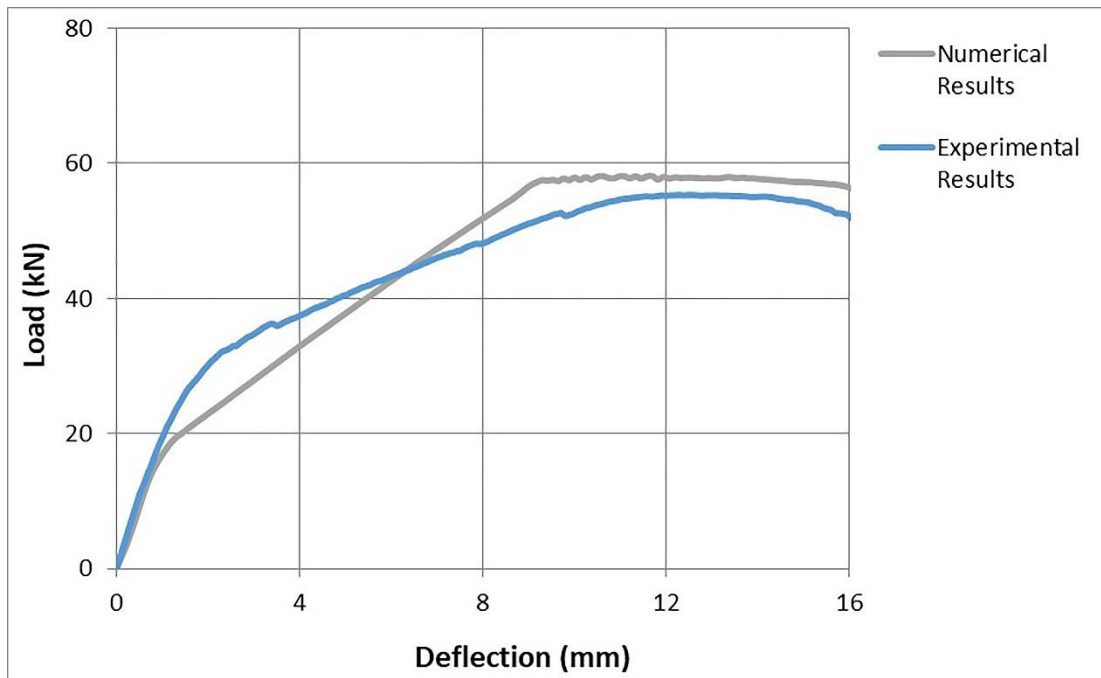
490   16a-d respectively.

491

492   **Fig.16a**

493
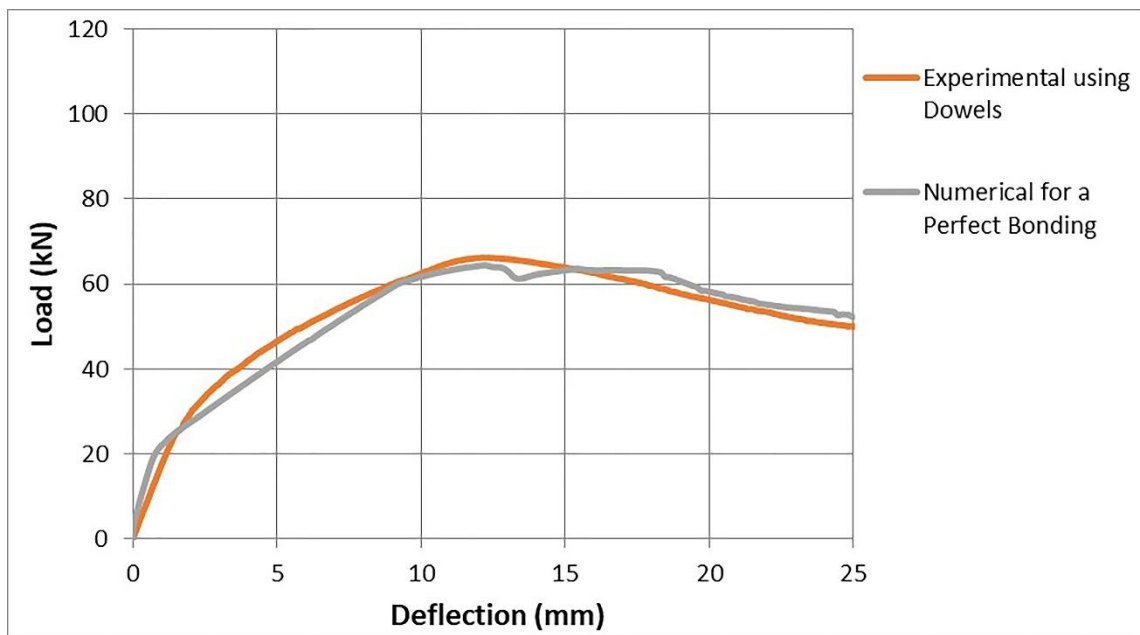
494

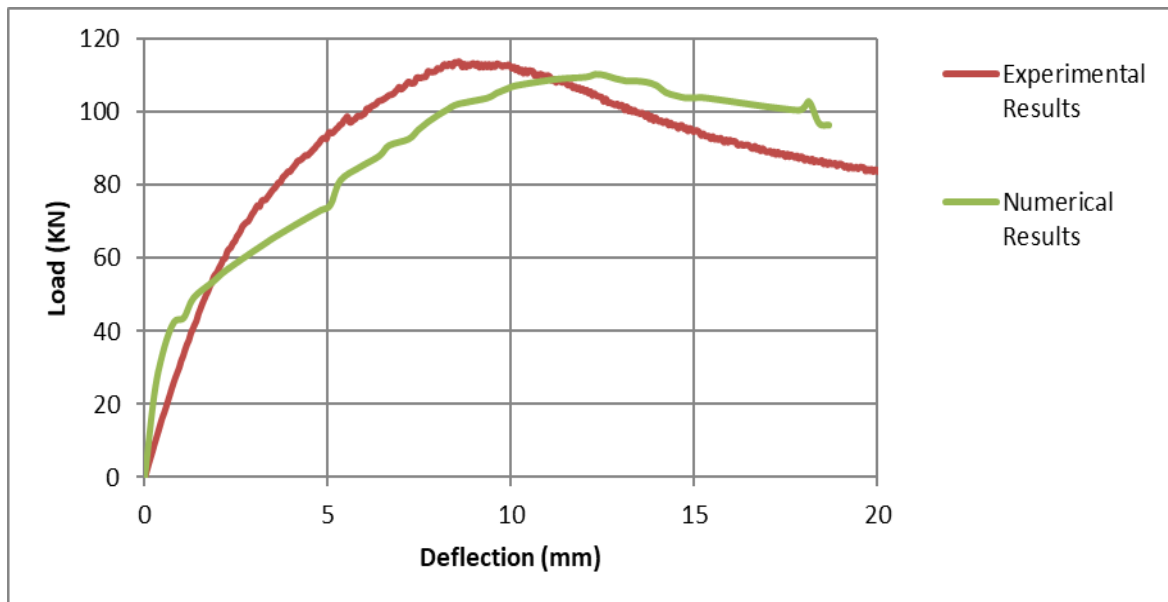495 **Fig.16b**

496

497 **Fig.16c**

498

Fig.16d

499

Fig. 16 Experimental versus numerical results for a) the control beam P b) the beam

strengthened with layers U c) the beams strengthened with beams and dowels D d) the beams

strengthened with jackets

The results of Fig. 16a indicate that there is a very good agreement between the

experimental and the numerical results for the control beams. For the strengthened beams with

layers (Fig. 16b), the use of contact elements with coefficient of friction equal to 1 and cohesion

equal to 1.8 MPa leads to numerical results very close to the experimental. In case of the

strengthened specimens with dowels (Fig. 16c), the assumption of perfect bonding at the

interface of the beam of the numerical model shows a remarkable agreement with the beam of

the experimental investigation with the addition of dowels. Finally, a good agreement between

the experimental and the numerical results can be observed for the beams strengthened with

jackets. The load carrying capacity of the numerical model (110 kN) is very close to the

respective experimental value (114.5 kN), while slightly higher stiffness is obtained

numerically.

514　　　　　　The failure mode of the examined numerical models at the point where the load capacity

515　　has been reduced to 80% of the maximum load, is presented in Figures 17a-c.
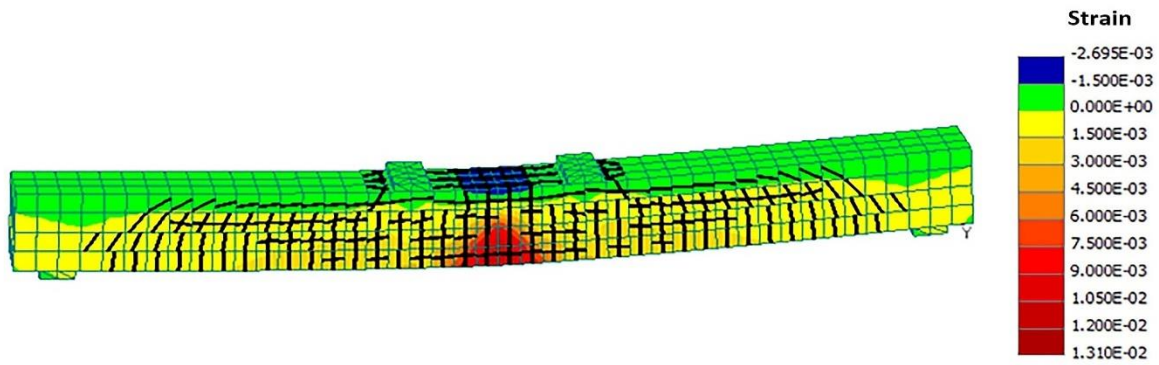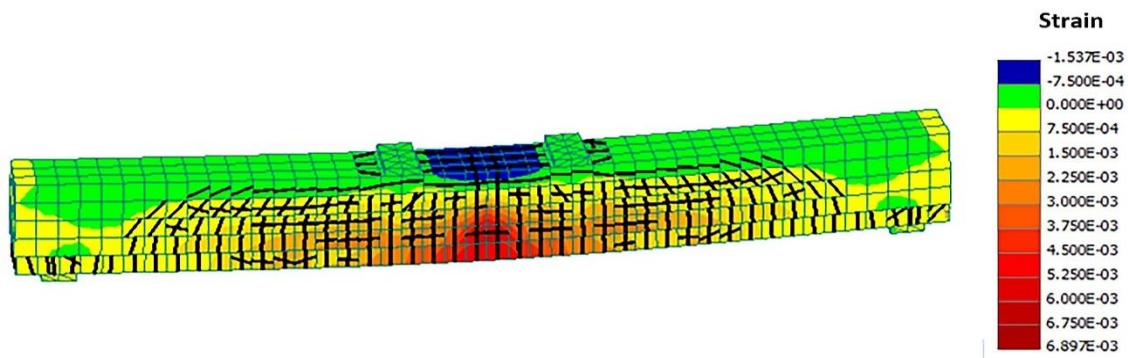

516

517　**Fig.17a**
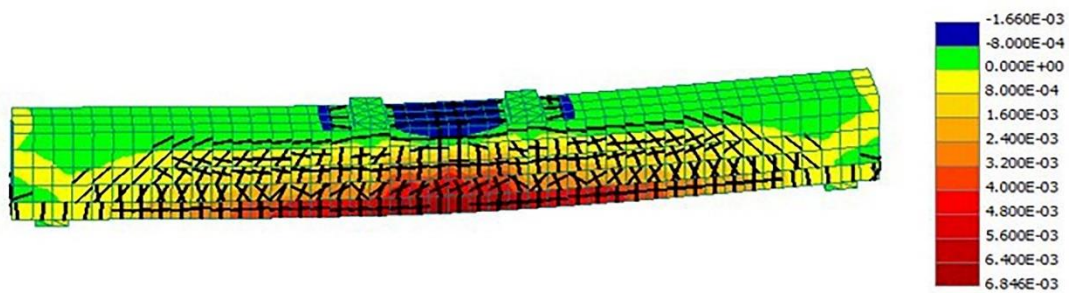

518

519　**Fig.17b**

520

521　**Fig.17c**

522

Fig.17d

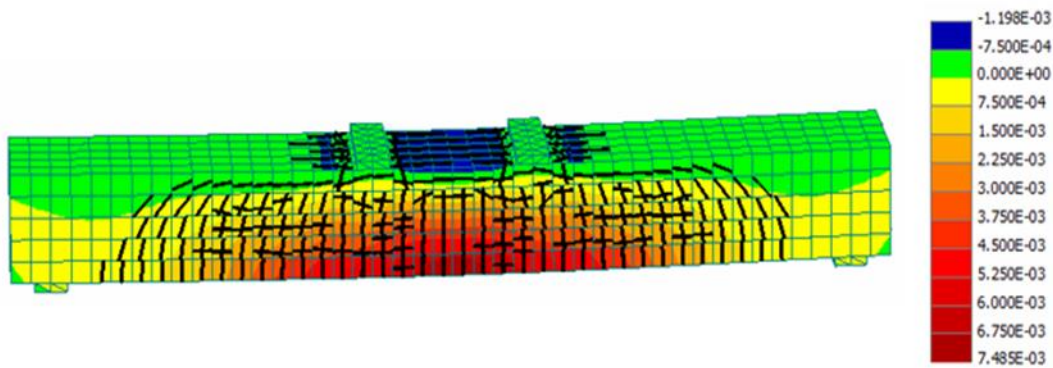**Fig. 17** Failure mode of a) control beam b) beam strengthened with UHPFRC layer c) beam strengthened with UHPFRC layers and perfect bonding d) beam strengthened with Jacket

The results of Figure 17 indicate that the crack patterns of the numerical models are in a very good agreement with the failure mode observed from the experimental investigation, with high values of strain concentration at the tensile side of the beams and localization of the damage in the middle of the span. Also, in Figures 17a-c high values of strain at the compressive side can be distinguished, similar to the experimental observations where failure at the compressive side occurred (Figures 10a-g).From the experimental results it is evident that the use of dowels results in better bonding between UHPFRC and RC with lower values of slip, while the formation of cracks is delayed. From Figure 16c and the comparison between the numerical results for monolithic connection and the experimental results using dowels, it is clear that when dowels are used, the response of the strengthened beams approaches the respective monolithic of the beam of the numerical investigation, as assumed for the application of the model. In addition, as can be seen in Figure 17c, for a monolithic connection, the strain is distributed along the whole length of the beam and is not concentrated on a small area of the examined specimens. This allows the material of the layer (UHPFRC) to be better utilized and the crack localization to be delayed leading to higher load capacity and enhanced

541 structural performance, highlighting the beneficial effect of the use of dowels at the UHPFRC-

542 to-concrete interfaces.

543 **4. Conclusions**

544 The present research focused on the investigation of new techniques for the application

545 of UHPFRC as strengthening material without the use of additional steel bars in the

546 strengthening layers, aiming to offer improved structural performance. The first examined

547 technique focused on the investigation of the effectiveness of dowels at the interface between

548 UHPFRC and concrete for the strengthening of RC beams and the second technique

549 investigated the performance of strengthened beams using three-side UHPFRC jackets.

550 Extensive systematic experimental work has been conducted followed by a numerical

551 study focused on the effect of the interface conditions. The following conclusions can be

552 drawn:

553 • The contribution of UHPFRC layer (without dowels) can be efficient for the serviceability

554 limit state. The experimental results of the present study recorded high values of slip after this

555 state, which can lead to debonding and lower load carrying capacity.

556 • Dowels at the interface between UHPFRC and RC result in better bonding, with lower

557 interface slip values preventing de-bonding. Also, dowels delay the formation of cracks.

558 • The addition of dowels at the interface leads to enhanced load carrying capacity of the

559 strengthened beams. The experimental results of the present study indicated an increase of

560 21.5% of the load carrying capacity when dowels were used at the interface. The respective

561 increase without the use of dowels was only 1.5%.

562 • The addition of dowels at the interface leads to better distribution of the stresses along the

563 length of the strengthened elements.

- Superior performance between the examined techniques was achieved for strengthening with three-side jackets. In this case, the load carrying capacity was increase by 110% and the stiffness by 270%.

- A remarkable agreement was identified from the comparison of the experimental results using dowels with the numerical results considering monolithic connection at the interface between UHPFRC and RC.

From the results of the present study it is clear that both, the addition of dowels and jackets, are effective techniques which can improve the performance of the strengthened elements. The selection of the appropriate technique should be depended on the desired outcome of the technique to increase the strength, the stiffness or both.

The use of dowels is a technique which should be taken into consideration to reduce the effect of imperfections during the roughening of the interface and to eliminate the risk of premature de-bonding of the strengthening layer. The construction of jackets on the other hand, should be preferred in heavily damaged RC members or in cases where the load carrying capacity and stiffness need to be significantly increased.

Acknowledgements

REFERENCES

[1] Ferrara, L., Ozyurt, N., Di Prisco, M., "High mechanical performance of fibre reinforced cementitious composites: the role of "casting-flow induced" fibre orientation", Materials and Structures, 2011, 44 (1), 109-128.

586   [2] Nicolaides, D., Kanellopoulos, A., Petrou, M., Savva P., Mina A., "Development of a new

587   Ultra High Performance Fibre Reinforced Cementitious Composite (UHPFRCC) for impact

588   and blast protection of structures", Construction and Building Materials, 2015, 95, 667-674

589   [3] Paschalis, S.A., Lampropoulos, A., "Fiber content and curing time effect on the tensile

590   characteristics of Ultra High Performance Fiber Reinforced Concrete (UHPFRC)", Structural

591   Concrete, 2017, 18 , 577-588

592   [4] Paschalis, S.A., Lampropoulos A., "Ultra High Performance Fiber Reinforced Concrete

593   Under Cyclic Loading", ACI Materials Journal, 2016, 113 (4), 419-427

594   [5] Kang, S.T., Kim, J.K., "The relation between fiber orientation and tensile behavior in an

595   Ultra High Performance Fiber Reinforced Cementitious Composites (UHPFRCC)", Cement

596   and Concrete Research, 2011, 41(10), 1001-1014

597   [6] Tsioulou, O., Lampropoulos, A., Paschalis, S.A., "Combined Non-Destructive Testing

598   (NDT) method for the evaluation of the mechanical characteristics of Ultra High Performance

599   Fibre Reinforced Concrete (UHPFRC)", Construction and Building Materials, 2017, 131, 66-

600   77.

601   [7] Vaitkevicious V., Serelis E., Vaiciukyniene, Raudonis V.,Rudzionis Z., "Advanced

602   mechanical properties and frost damage resistance of ultra-high performance fibre reinforced

603   concrete", Construction and Building Materials, 2016, 126, 26-31

604   [8] Bruhwiler, E., Denarie E., "Rehabilitation of concrete structures using Ultra-High

605   Performance Fibre Reinforced Concrete", The Second International Symposium on Ultra High

606   Performance, 2008, Kassel, Germany

607   [9] Al-Osta, M., Isa, M., Baluch, M. & Rahman, M., 2017. Flexural behaviour of reinforced

608   concrete beams strengthened with ultra-high performance fiber reinforced concrete.

609   Construction and Building Materials, Volume 134, pp. 279-296.

610   [10] Safdar M., Takashi Matsumoto T., Kakuma K, Flexural behavior of reinforced concrete

611   beams repaired with Ultra High Performance Fiber Reinforced Concrete (UHPFRC),

612   Composite Structures, 2016, 157, 448-460.

613   [11] Lampropoulos, A., Paschalis, S.A., Tsioulou O., Dritsos S., "Strengthening of reinforced

614   concrete beams using ultra high performance fibers reinforced concrete (UHPFRC)",

615   Engineering Structures, 2015, 106, 370-384.

616   [12] Paschalis, S.A., Lampropoulos, A., Tsioulou, O., "Experimental and numerical study of

617   the performance of Ultra High Performance Fiber Reinforced Concrete–Reinforced Concrete

618   for the flexural strengthening of full scale members", Construction and building materials,

619   2018, 186, 351-366.

620   [13] Trucy l., Dobrusky S., Bonnet E., Ultra-high performance shotcrete: yes we can!,

621   proceedings of UHPFRC 2017 Designing and Building with UHPFRC: New large-scale

622   implementations, recent technical advances, experience and standards, 2017, pp 154 – 163,

623   [14] Ductal, Innovation: Ductal Shotcrete the first sprayed UHPC Accessed on 25-11-2019 at

624   https://www.ductal.com/en/engineering/innovation-ductalr-shotcrete-first-sprayed-uhpc

625   [15] Skazlic M., Skazlic Z. ; and J. Majer J., Application of High Performance Fibre

626   Reinforced Shotcrete for Tunnel Primary Support, 10th International Conference on Shotcrete

627   for Underground Support, Whistler, 2006. p. 206-214.

628   [16] Greek Organization for Seismic Planning and Protection, Greek Retrofitting Code

629   (GRECO), Athens, (in Greek), 2013

630   [17] Paschalis, S.A, Lampropoulos, A., "Mechanical performance and cost correlation of Ultra

631   High Performance Fiber Reinforced Concrete (UHPFRC)", 19th Congress of IABSE

632   Stockholm, 2016, Stockholm, Sweden

633   [18] Hellenic Technical Specification, Placement Dowels in Concrete Elements, Greek

634   Ministry of Environment and Energy, 2009, (In Greek)

635   [19] BS EN 12390-3:2009, Testing hardened concrete-Part 3: Compressive strength of test

636   specimens

637   [20] Greek Retrofitting Code, (GRECO) Greek Organization for Seismic Planning and

638   Protection, Athens, Greek Ministry for Environmental Planning and Public Works, 2013 (in

639   Greek)

640   [21] fib Bulletin No 43, Structural Connections for precast concrete buildings, Lausanne,

641   International Federation for Structural Concrete, 2008

642   [22] Tsioulou, O., Lampropoulos, A., Dritsos, S., Experimental investigation of interface

643   behavior of RC beams strengthened with concrete layers, Construction and Building Materials,

644   40: (2013), 50-59.

645   [23] Cervenka,V., Jendele, L., Cervenka, J., ATENA Program Documentation: Part 1 Theory,

646   Prague, Czech Republic,2013

647   [24] BS 4449:2005 Steel for the reinforcement of concrete. Weldable reinforcing steel. Bar,

648   Coil and Decoiled product. Specification, BSI, (2005)

649   [25] CEB Bulletin No. 213/214, CEB-FIP Model Code 90. International Federation for

650   Structural Concrete, Lausanne, (2013)

651

652